A heterodyne dispersion interferometer for wide bandwidth density measurements on DIII-D[a]

T. Akiyama[1,b], M.A. Van Zeeland[2], R.L. Boivin[2], T.N. Carlstrom[2], A. Chavez[2], C.M. Muscatello[2], R. O'Neill[2], J. Vasquez[2], M. Watkins[2], W. Martin[2], A. Colio[3], D.K. Finkenthal[3], D.L. Brower[4], J. Chen[4], W.X. Ding[4], and M. Perry[5]

[1] *National Institute for Fusion Science, 322-6 Oroshi-cho, Toki-shi, Gifu 509-5292, Japan*
[2] *General Atomics, P.O. Box 85608, San Diego, California 92186-5608, USA*
[3] *Palomar College, San Diego, California 92069, USA*
[4] *University of California Los Angeles, Los Angeles, California 90095, USA*
[5] *Cal State University, San Marcos, San Marcos, California, 92096, USA*

In order to improve both the density and particularly the temporal resolution beyond previous dispersion interferometers (DI), a heterodyne technique based on an acousto-optic (AO) cell has been added to the DI. A 40 MHz drive frequency for the AO cell allows density fluctuation measurements into the MHz range. A CO_2 laser based heterodyne DI (HDI) installed on DIII-D has demonstrated that the HDI is capable of tracking the density evolution throughout DIII-D discharges, including disruption events and other rapid transient phenomena. The data also show good agreement with independent density measurements obtained with the existing DIII-D two-color interferometer. The HDI line-integrated density resolution sampled over a 1s interval is ~9×10^{17} m^{-2}. Density fluctuations induced by MHD instabilities are also successfully measured by the HDI.

I. INTRODUCTION

Measurement of the electron density (n_e) in fusion plasmas via interferometry is a common and indispensable technique used worldwide. Despite being common, however, interferometry has intrinsic disadvantages such as potential fringe jump errors and measurement errors caused by mechanical vibrations. Fringe jump errors are often caused by refraction of the probe beam in a plasma which leads to loss of signal. Since the phase shift ϕ induced by fusion plasmas ($\phi = \lambda r_e \int n_e\, dl$, where r_e=2.82×10^{-15} m is the classical radius of electron, λ is the wavelength of a probe beam, and l is the path length in a plasma), which is proportional to λ, is typically larger than 2π, an interruption of a detected signal by a beam displacement from a detector leads to ambiguity of 2π in the evaluated phase shift. This ambiguity can appear as a jump of the electron density. Changes in the beam path length (Δd) due to mechanical vibrations will also cause a phase shift ($2\pi\Delta d/\lambda$) that, depending on wavelength, can be orders of magnitude larger than that from the plasma. As beam refraction in a plasma is roughly proportional to λ^2, mid-IR wavelengths such as that of CO_2 lasers (~9-10 μm) are suitable to minimize refraction while still obtaining measurable plasma induced phase shifts. Unfortunately, as discussed above, the phase

shift caused by mechanical vibrations become larger for the shorter wavelengths and can dominate that from the plasma. To overcome this issue, and actually measure both the plasma and vibration induced phase shift, a two-color interferometer which uses two laser sources with different wavelengths sharing the same line of sight in a plasma is usually adopted[1]. Based on the different dependencies on the wavelength, the phase shifts caused by the plasma and that from mechanical vibrations can be separated by resolving separately the phase shifts at each wavelength.

While a dispersion interferometer (DI)[2] is basically a two-color interferometer, the interferometer configuration and the approach with which the vibration induced phase shift is removed, are different. The DI is equipped with one laser source and the second color is generated with a nonlinear crystal at half the fundamental laser wavelength. The fundamental and the second harmonic components have essentially the same optical paths and a second nonlinear crystal generates a separate second harmonic component after passing through a plasma. The fundamental component is removed by a filter and the interference between two second harmonic components, which are generated before and after passage through the plasma, is detected. Since the two beams propagate along the same beam path, the phase shift in the interference signal is attributed to the different index of refraction between the fundamental and the second harmonic component. Any phase shift due to path length changes cancels out in the measurement and post-detection processing is not required to isolate the plasma effect. Consequently, total number of
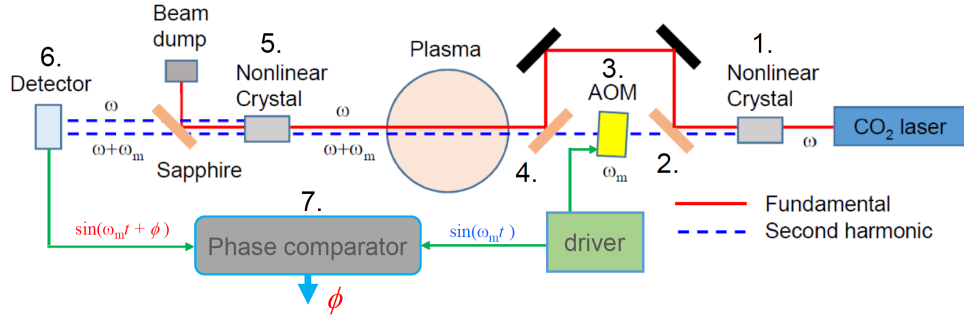
FIG 1. Principle of the heterodyne interferometer

fringes can be reduced significantly, which can decrease the risk associated with fringe jumps.

One challenge of the DI approach is phase extraction. Indeed, the original DI was a homodyne interferometer[2], which is dependent on the detected intensity to evaluate the phase. Complications to the homodyne approach include for example: laser oscillation instability, beam displacements caused by refraction in a plasma or vibrations, and electrical noise. Hence several approaches have been tested to solve this disadvantage. One such approach is the phase modulation method[4-8]. In this approach, a phase modulation is added to one wavelength component with an electro-optic (EO) cell or a photoelastic modulator (PEM) so that the phase shift can be evaluated independently of the detected intensity. The achieved density and the time resolution with this approach are typically sufficient for density control in fusion devices (~50 kHz) and, in fact, this DI is being proposed to ITER as a backup system[9] to toroidal interferometer polarimeter (TIP)[1]. Although the modulation frequency of EO cells is high, at 250 kHz, thermal instability of EO cells for infrared wavelengths has been reported[4]. Hence the EO cell is not suitable for long pulse measurements. While PEMs are thermally stable, the modulation frequencies are typically 50 kHz at most and the bandwidth is not sufficient for density fluctuation measurements.

The heterodyne technique discussed here uses an acousto-optic (AO) cell and is capable of a wide bandwidth measurements, potentially up to 100 MHz. Proof-of-principle table top heterodyne DI experiments were conducted recently and are discussed in Reference [10]. This work expands on the original tests and includes the first heterodyne dispersion interferometer (HDI) measurements of both the equilibrium density and instability-induced density fluctuations on the DIII-D tokamak. In this paper, the principle of the heterodyne DI is explained in section II and the optical system of the HDI on DIII-D is described in the section III. Measurements of the equilibrium electron density and density fluctuations are shown in section IV including comparison with the standard two-color interferometer on DIII-D. Section IV gives a brief summary.

II. PRINCIPLE OF HETERODYNE DISPERSION INTERFEROMETER

Despite being common for standard two-color interferometers, the acousto-optic-cell-based heterodyne technique is not common for DIs and was first proposed by Brower[11]. Figure 1 shows a schematic view of the HDI, the sequential process of which is as follows:
1. Second harmonic generation by a nonlinear crystal.
2. Separation of fundamental and second harmonic components by a beam splitter.
3. Frequency shift by $\omega_m/2\pi = 40$ MHz with the AO cell to one of wavelength components (second harmonic in Fig. 1)
4. Recombination of two components by a beam combiner and propagation through the plasma.
5. Second harmonic generation from the fundamental with another nonlinear crystal after the plasma.
6. Detection of the interference signal $\sin(\omega_m t + \phi)$ between two second harmonics, which includes the phase shift ϕ by the plasma.
7. Phase comparison between $\sin(\omega_m t + \phi)$ and the AO cell drive signal $\sin(\omega_m t)$ with a phase demodulator to extract the phase shift ϕ.

III. OPTICAL SETUP ON DIII-D

The majority of HDI optics and electronics components are placed in a dedicated laser room and the probe beam propagates to the DIII-D tokamak along a fully enclosed beam duct. The total double-pass path length is approximately 100 m, which is comparable to that expected on ITER[9]. Due to the long beam path and proximity of several components to the tokamak, which causes significant motion during a discharge, active feedback alignment of the system is essential. To maintain overall system alignment and to ensure adequate interference signal, the HDI uses a feedback alignment system developed for the ITER TIP prototype[2,3].

Figure 2 shows the HDI optical table arrangement. The output power and the wavelength of the laser (GEM Select 50, Coherent) are 50 W and 10.591 μm (10P20), respectively. To avoid damage of the AR coating on the nonlinear crystal OP-GaAs (Physical Sciences Inc.), only 27 W of the available 50 W is used. The beam power at each position on the table is shown in Table 1. The laser beam is focused at the nonlinear crystal (beam radius ω of 0.17 mm) to increase the efficiency of the second harmonic generation. The generated second harmonic power at the first crystal is
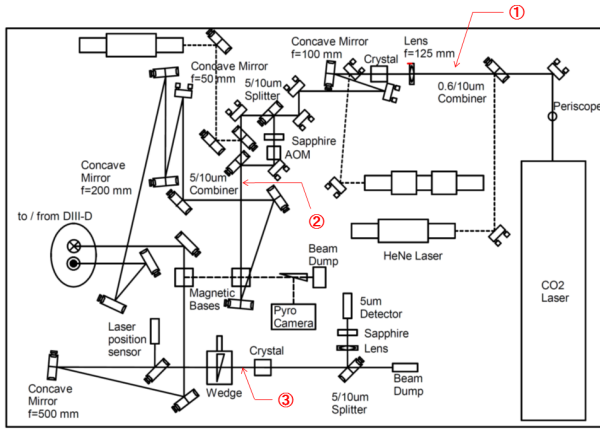
FIG 2. Arrangement of optics of the heterodyne dispersion interferometer

Table 1. Beam power at each position

Position	①	②	③
10.6 μm	27 W	7.3 W	0.3 W
5.3 μm		9 mW	-
Memo	Only half of the maximum power is used.	10.6 μm is absorbed by ZnSe beam splitter/ combiners	5.3 μm was too small to measure with a power meter.

9 mW. After beam collimation, the fundamental and the second harmonic components are separated with a ZnSe beam splitter. The second harmonic component is reflected

Beam transmission to DIII-D is shown in Fig. 3. The beam path is enclosed with 150mm diameter aluminum pipes for laser safety and the diameter of the bending mirrors, which are enclosed in aluminum boxes, is 150 mm. The probe beam is injected radially into DIII-D along the device midplane through a double BaF_2 window. A corner cube reflector mounted inside the vacuum vessel displaces the probe beam vertically and the return beam is guided to the laser room through the same optics and beam duct.

Between discharges and without feedback alignment enabled, the return beam in the laser room typically jitters by several millimeters over second level intervals due to small vibrations of mirrors along the 100 m beam transmission line. Over hour timescale intervals, the return beam can move by centimeters due to thermal changes of the optical components. During a plasma discharge, energization of the central solenoid causes even larger mechanical vibrations, leading to total loss of the return beam back in the laser room when feedback alignment is disabled. While the OP-GaAs nonlinear crystal has relatively high efficiency for second harmonic generation, the incident face is small (1 mm×5 mm). Although the laser beam is focused on the crystal, movements of the return laser beam must be minimized as small as possible to prevent clipping and a reduction in interference signal. Hence, the mirror in front of the vacuum window was mounted to a tip-tilt piezo stage and the mirror angle was
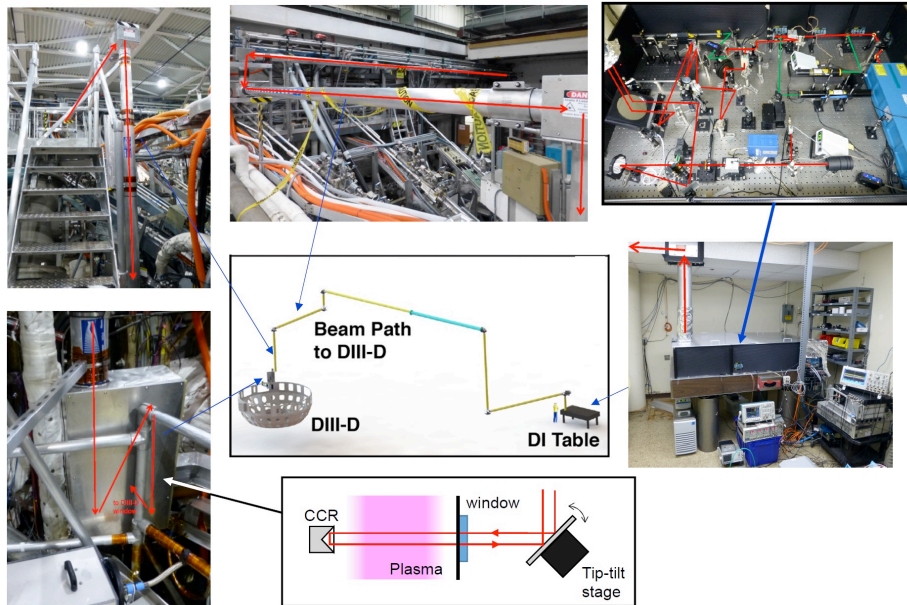

FIG 3. Beam transmission of the heterodyne dispersion interferometer on DIII-D.

and the remaining fundamental component in the reflected beam is removed with a saphire plate. The second harmonic component is injected into the AO cell and the frequency is shifted by 40 MHz. The frequency-shifted second harmonic and fundamental components are combined again with a ZnSe beam combiner. The collinear combined beams are sent to a beam expander with an expansion ratio of 4 (=200 mm/50 mm) and the fundamental component is collimated. The beam radius before being sent to DIII-D is approximately 20 mm.

actively controlled by using a signal from a position sensor in the laser room. The position sensor monitors the position of a portion of the return beam split off in front of the second nonlinear crystal. This technique, developed for the TIP system[2,3], allows the HDI to maintain transmission through the crystal and sufficient interference signal amplitude. It is estimated that motion of the laser spot on the crystal is minimized to less than 0.5 mm when the opical feedback system is activated.

After second harmonic generation in the final nonlinear crystal, the two second harmonic components only, which are generated before and after the plasma, are reflected by the ZnSe beam splitter and the interference signal between two second harmonics is detected. The sapphire plate shown in Figure 2 eliminates the remaining fundamental component in front of the detector (PVMI-8, VIGO). The detected beat signal with a frequency of 40 MHz and with an amplitude of 0.25 V is input to the digital phase demodulator (DPD) developed by Palomar Scientific Instruments for the ITER TIP project[1]. The phase difference between the detector and the reference signal from AO cell driver is analyzed using the DPD with 1 MS/s bandwidth and the data are stored at 1 MS/s.

Essential to accurate vibration cancellation by the HDI is precise overlap of the fundamental and the second harmonic components. If the two beams have a relative displacement, even minor differences in the mechanical vibrations and perturbations by air or water vapor cause measureable phase errors. To ensure adequate co-alignment of the two beams, the overlap of the full path return beams as well as just after beam combination were measured with an infrared camera on the optical table. This Pyrocam based approach, also originally developed for the ITER TIP system[2,3], allows fine tuning of the beam overlap not possible with traditional CO_2 laser thermal detection plates.

IV. MEASUREMENT RESULTS ON DIII-D

A. Resolution of the HDI

An example line-integrated density measured by the HDI during a DIII-D H-mode discharge is shown in Figure 4. The typical HDI line-integrated density resolution, defined as the standard deviation over a 1s interval before or after a plasma, is 9×10^{17} m^{-2}., which is comparable to that of the two-color interferometer with the same beam path[3]. If one considers application to ITER, the total path length in a plasma for a tangential line of sight is ~24 m. Thus, the achieved line-integrated density resolution corresponds to a line-averaged electron density of 3.8×10^{16} m^{-3} on ITER. This demonstrated density resolution is smaller than 0.1% of the expected electron density during the flat-top phase (3.8×10^{19} m^{-3} - 4×10^{20} m^{-3}) in a standard H-mode discharge on ITER.

Phase drift is sometimes observed. The drift typically coincides with periods during which the laser room air conditioner is in on. One possible reason for the drift is inhomogeneities of the air temperature or the density around the AO cell. Since the beam paths of the fundamental and the second harmonic components are different around the AO cell, relative phase shifts in this portion (around 60 cm-long) cannot be cancelled without adding a second reference detector as in Reference [1]. As discussed in [1], the other possibility is amount of water vapor, which determines the refractive index and dispersion of the air. The 5.3 μm second harmonic component is close to a water vapor absorption line and the refractive index of the air at 5.3 μm can be strongly affected by changes of air humidity induced by the air conditioner. One solution to this issue is to use an
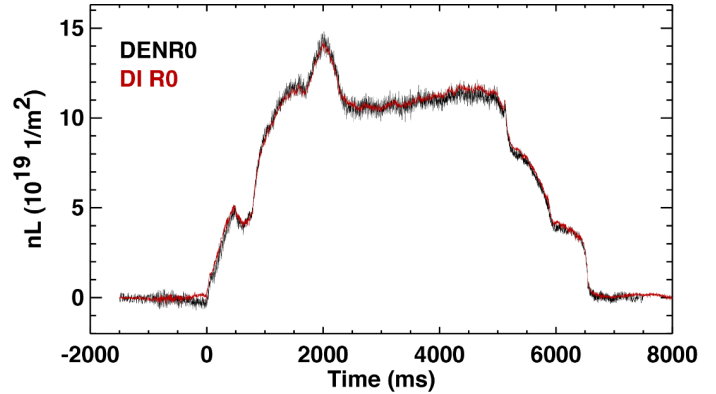

FIG 4 . The line-integrated electron densities measured with the radial two-color interferometer ("DENR0") and with the HDI ("DI R0"). They have similar path length in a plasma.

oscillation line of 9.552 μm (9P20), which has similar output power as that of 10P20. Its second harmonic, 4.776 μm is outside the absorption line and should be less perturbed by water vapor.

B. Comparison with the DIII-D two-color interferometer

Figure 4 also shows a comparison of the line-integrated electron density measured by the HDI to that measured by the DIII-D traditional two-color (10.59 μm CO_2/3.39 μm HeNe) laser interferometer which is on a similar path and shares the inner wall corner cube reflector. The measured electron density with the HDI shows good agreement to that measured with the two-color interferometer throughout the discharge. Even when large mechanical vibrations occur during the current ramp-up and ramp-down phase, the active feedback control works and degradation of the density resolution was not observed. It was also found that disruptions, H-mode transitions and ELMs on DIII-D do not interrupt the HDI electron density measurement.

C. Electron density fluctuation measurement

Taking advantage of the wide bandwidth (limited only by the 40MHz AO drive frequency), analysis of density fluctuations with the HDI are also carried out. Figure 5 shows the frequency spectrum of electron density fluctuations in an H-mode discharge measured with the HDI. In this discharge, density fluctuations, identified as tearing modes, were clearly observed at frequencies up to 100 kHz. In Fig. 5 (c), the spikey and broadband spectrum from 0 to 100 kHz is caused by ELMs. Sharp decrease and gradual recovery of the coherent fluctuations are observed around 25 kHz, 50 kHz, and 75 kHz. They are speculated to be caused by changes in the electron density or plasma rotation due to the ELMs. In addition to coherent fluctuations, relatively broadband density fluctuations up to 150 kHz appear from 4.2 to 4.4 s as shown in Fig. 5(d). These results clearly demonstrate the capability of the HDI as a high-frequency electron density fluctuation diagnostic.
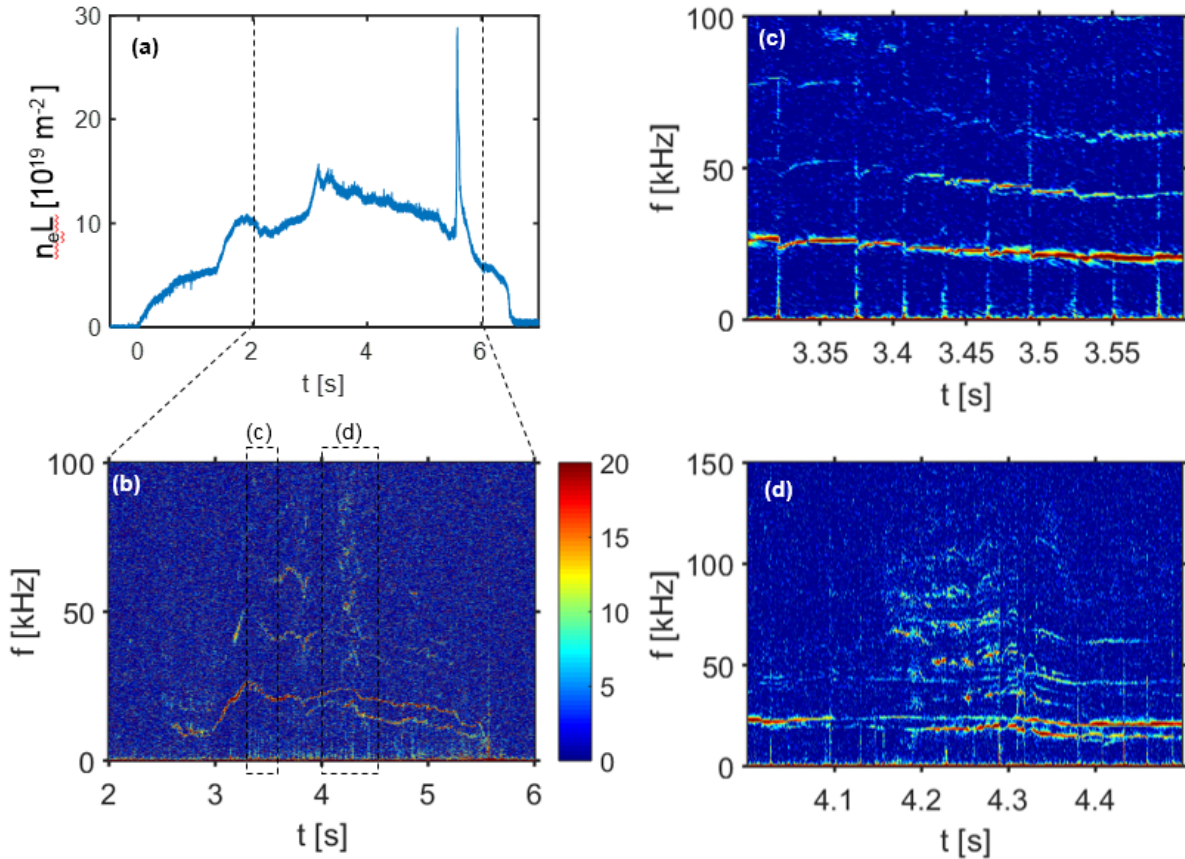
V. SUMMARY

A heterodyne dispersion interferometer for wide bandwidth electron density measurements in fusion plasmas has been installed and proven on the DIII-D tokamak with a comparable beam path length to that expected on ITER. Essential to the implementation was an active feedback alignment system, developed for the prototype toroidal interferometer and polarimeter system for ITER, which maintains alignment of the probe beam. The achieved line-density resolution is 9×10^{17} m^{-2}. The measured line-density also shows good agreement with that measured by the traditional two-color interferometer on DIII-D, even through disruptions. Additionally, density fluctuations have been successfully measured by the HDI.

Acknowledgements

Disclaimer

References

[1] M. A. Van Zeeland *et. al.*, Plasma Phys. Control. Fusion **59**, 125005 (2017).
[2] V.P. Drachev *et. al.*, Rev. Sci. Instrum. **64**, 1010 (1993).
[3] M.A. Van Zeeland *et.al.* Rev. Sci. Instrum. In submission (2018)
[4] P. A. Bagryansky *et al.*, Rev. Sci. Instrum. **77**, 053501 (2006).
[5] T. Akiyama *et. al.*, Rev. Sci. Instrum. 85 11D301 (2014).
[6] J. Knauer *et al.*, EUROFUSION WPS1-PR(16) 16154
[7] K. J. Bruuner *et al.*, *submitted to this conference*
[8] H.X. Wang *et. al.*, Rev. Sci. Instrum. **88**, 103502 (2017).
[9] T. Akiyama *et. al.*, Rev. Sci. Instrum. **87** 11E133 (2016).
[10] T. Akiyama *et. al.*, Rev. Sci. Instrum. **87** 123502 (2016).
[11] Private communication.